CardiOvascular examination in awake Orangutans (Pongo pygmaeus pygmaeus): Low-stress Echocardiography including Speckle Tracking imaging (the COOLEST method)

Valérie Chetboul, Didier Concordet, Renaud Tissier, Irène Vonfeld, Camille Poissonnier, Maria Paz Alvarado, Peggy Passavin, Mathilde Gluntz, Solène Lefort, Aude Bourgeois, et al.

PLOS ONE

RESEARCH ARTICLE

CardiOvascular examination in awake Orangutans (*Pongo pygmaeus pygmaeus)*: Low-stress Echocardiography including Speckle Tracking imaging (the COOLEST method)

Valérie Chetboul[1,2]*, Didier Concordet[3], Renaud Tissier[2], Irène Vonfeld[1], Camille Poissonnier[1], Maria Paz Alvarado[1], Peggy Passavin[1], Mathilde Gluntz[1], Solène Lefort[1], Aude Bourgeois[4], Dylan Duby[4], Christelle Hano[4], Norin Chai[4]

1 École nationale vétérinaire d'Alfort, CHUVA, Unité de Cardiologie d'Alfort (UCA), Maisons-Alfort, France, **2** Univ Paris Est Créteil, INSERM, IMRB, Créteil, France, **3** Intheres, Université de Toulouse, INRA, ENVT, Toulouse Cedex 3, France, **4** Ménagerie, le Zoo du Jardin des Plantes, Muséum National d'Histoire Naturelle, Paris, France

* valerie.chetboul@vet-alfort.fr

OPEN ACCESS

Citation: Chetboul V, Concordet D, Tissier R, Vonfeld I, Poissonnier C, Alvarado MP, et al. (2022) CardiOvascular examination in awake Orangutans (*Pongo pygmaeus pygmaeus)*: Low-stress Echocardiography including Speckle Tracking imaging (the COOLEST method). PLoS ONE 17(1): e0254306. https://doi.org/10.1371/journal.pone.0254306

Editor: Muhammad Mansoor Mohiuddin, University of Maryland School of Medicine, UNITED STATES

Received: June 25, 2021

Accepted: December 29, 2021

Published: January 24, 2022

Data Availability Statement: All relevant data are within the manuscript and its Supporting Information files.

Funding: The author(s) received no specific funding for this work.

Competing interests: The authors have declared that no competing interests exist.

Abstract

Introduction

Cardiovascular diseases have been identified as a major cause of mortality and morbidity in Borneo orangutans (*Pongo pygmaeus pygmaeus*). Transthoracic echocardiography is usually performed under anesthesia in great apes, which may be stressful and increase risks of peri-anesthetic complications in case of cardiac alteration. The aim of the present pilot study was hence to develop a quick and non-stressful echocardiographic method (i.e., the COOLEST method) in awake Borneo orangutans (CardiOvascular examination in awake Orangutans: Low-stress Echocardiography including Speckle Tracking imaging) and assess the variability of corresponding variables.

Materials and methods

Four adult Borneo orangutans trained to present their chest to the trainers were involved. A total of 96 TTE examinations were performed on 4 different days by a trained observer examining each orangutan 6 times per day. Each examination included four two-dimensional views, with offline assessment of 28 variables (i.e., two-dimensional (n = 12), M-mode and anatomic M-mode (n = 6), Doppler (n = 7), and speckle tracking imaging (n = 3)), representing a total of 2,688 measurements. A general linear model was used to determine the within-day and between-day coefficients of variation.

Results

Mean±SD (minimum-maximum) images acquisition duration was 3.8±1.6 minutes (1.3–6.3). All within-day and between-day coefficients of variation but one (n = 55/56, 98%) were <15%, and most (51/56, 91%) were <10% including those of speckle tracking systolic strain variables (2.7% to 5.4%).

Discussion

Heart morphology as well as global and regional myocardial function can be assessed in awake orangutans with good to excellent repeatability and reproducibility.

Conclusions

This non-stressful method may be used for longitudinal cardiac follow-up in awake orangutans.

Introduction

Cardiovascular diseases have been identified as a major cause of mortality and morbidity in great apes including Borneo orangutans (BO, *Pongo pygmaeus pygmaeus*) under managed care [1]. According to a study based on the North American Orangutan Species Survival Plan, up to 20% of adult orangutan deaths housed in United States and Canadian zoos and private collections between January 1980 and March 2008 were of cardiovascular origin [1]. Based on published reports and analysis of Species Survival Plan necropsy data, orangutans are known to be affected by miscellaneous heart diseases including congenital cardiac defects [2, 3], cardiomyopathies [1, 4], and viral myocarditis [1, 5, 6]. The most common heart disease is known as fibrosing cardiomyopathy, characterized by a scattered pattern of myocardial fibrosis with atrophy and hypertrophy of cardiac myocytes, absent or mild inflammation, and no apparent etiology or associated diseases [1].

However, the *antemortem* diagnosis of such heart diseases remains challenging, partly because most of them are responsible for sudden death without prior cardiovascular clinical signs, although congestive heart failure may sometimes develop [1]. Additionally, complementary examinations are considered to be difficult to perform without general anesthesia in these species [1]. Heart diseases in orangutans are therefore currently mainly diagnosed by necropsy and histopathological examinations, and cardiology knowledge in this species remains limited.

Transthoracic echocardiography (TTE) has become a major non-invasive imaging tool for the *antemortem* diagnosis of heart diseases both in humans and various animal species, allowing qualitative description of cardiac abnormalities and quantitative assessment of heart anatomy and function using combined two-dimensional (2D) mode, M-mode, and conventional Doppler modes. More recent advances in ultrasound technology with the introduction of specific imaging modalities, such as 2D speckle tracking imaging (STI), have provided several complementary parameters to assess global and regional myocardial performance [7]. Regarding great apes, a program called the Great Ape Heart Project (GAHP), based at Zoo Atlanta, has collected a database of echocardiograms and other medical information related to their cardiac health status, and has also provided relevant guidelines for the echocardiographic assessment of anesthetized great apes, including standardization of nomenclature, imaging techniques (M-mode, 2D mode, spectral and color flow Doppler modes), as well as echocardiographic measurements [8]. According to the GAHP report, the use of general anesthesia allows to perform thorough and reliable TTE examinations [8]. However, anesthetizing great apes may be stressful and risky not only for cardiac patients but also for healthy animals, which limits the frequency of follow-up TTE sessions. Anesthetic drugs may also influence some TTE variables [8]. Moreover, to the best of our knowledge, global and regional function

of the left ventricle (LV) has never been quantitatively evaluated using STI in great apes, including BO.

The aims of the present pilot prospective study were therefore 1) to develop and assess the feasibility of a quick and non-stressful TTE method (i.e., the COOLEST method) in awake captive BO (CardiOvascular examination in awake Orangutans: Low-stress Echocardiography including Speckle Tracking imaging), and then 2) to determine the intra-observer within-day (repeatability) and between-day (reproducibility) variability of the corresponding measurements.

Materials and methods

Animals

Four apparently healthy adult BO were involved in the study, i.e., 3 females (31, 14 and 51 years old; 74, 47 and 69 kg respectively; BO1, BO2 and BO3 respectively) and 1 male (12 years old; 55 kg; BO4). This study was approved by the Ethics Committee of the National Museum of Natural History. No anaesthesia nor invasive procedure were performed for the purpose of the study protocol, and all BO remained in their normal environment during the whole study period. The BO facilities at La Ménagerie, le zoo du Jardin des Plantes at the Museum National d'Histoire Naturelle (Paris, France), included five indoor enclosures with controlled access to an outdoor area. Furnitures in the indoor and outdoor enclosures added physical complexity to their environment (climbing structures, ropes, platforms). A staff of six keepers worked with the BO, with at least two being present on site each day. Additionally, three full time veterinarians were involved in the health care and welfare of these animals that were fed five times a day (at 9:00 a.m., 10:30 a.m., 12:00 a.m., 2:30 p.m., and 5:00 p.m) with Mazuri (Dietex France, Argenteuil, France) primate maintenance biscuits, vegetables, fruits, and browse. All BO also received enrichments (feeding, physical, and cognitive) on a daily basis. Lastly, they were involved in a daily medical and husbandry training by operant conditioning techniques. When they were successful at exhibiting the requested behaviour, the keeper produced a clicker sound as a secondary reinforcer and gave a reward (e.g., a piece of fruit) and verbal praise.

Transthoracic echocardiographic technique and measurements

Echocardiographic procedure of the COOLEST method (CardiOvascular examination in awake Orangutans: Low-stress Echocardiography including Speckle Tracking imaging). Transthoracic echocardiographic examinations were performed in the orangutans' indoor enclosure in the Ménagerie, le Zoo du Jardin des Plantes (Paris, France) using a portable cardiovascular ultrasound system (Vivid i, GE Healthcare, 9900 Innovation Drive, Wauwatosa, WI 53226, USA) equipped with a 3S phased-array transducer (1.5–3.5 MHz).

Animal training for the TTE procedure was based on operant conditioning with exclusively positive reinforcement. Orangutans were first trained to sit and present their chest to the trainers against the enclosure mesh with their arms up. They were then desensitized to the ultrasound coupling gel (i.e., were trained for gel application on their thorax without reacting to the procedure) that was generously applied on the thorax through the enclosure mesh, and thereafter to the probe placement on their thorax. After three months of training, the four BO were easily conditioned to stay in the optimal position during several minutes for acquisition of images and video loops.

All transthoracic echocardiograms and corresponding measurements were performed by one single observer (VC), diplomate of the European College of Veterinary Internal Medicine (Cardiology), who was trained to the procedure during five sessions of trial before the

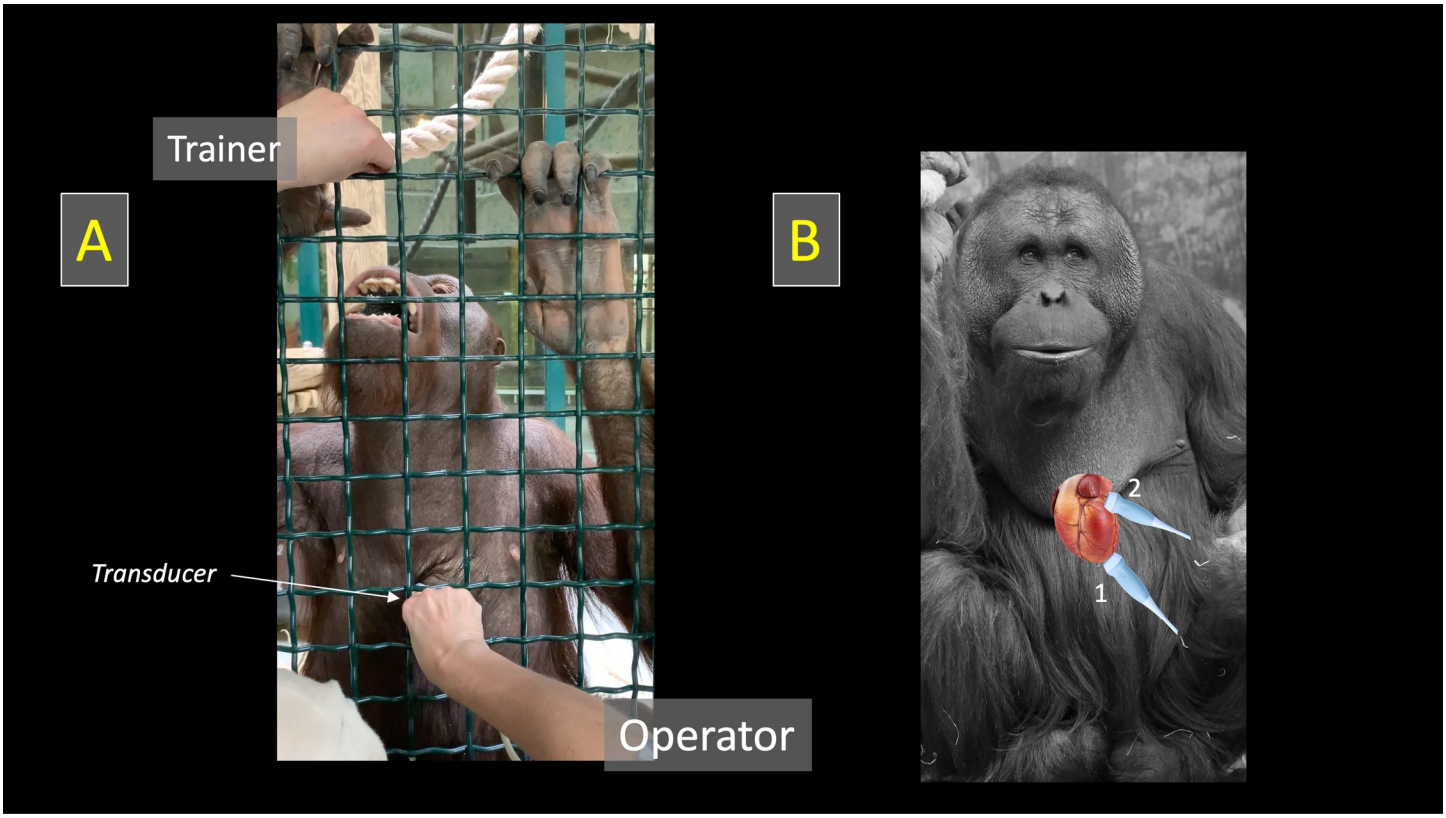

Fig 1. Orangutan positioning for echocardiographic examination and probe placement. Orangutan positioning for echocardiographic examination (A) and probe placement (B) for obtaining the apical long-axis views (1) and the parasternal short-axis view at the level of the aortic valve (2). *Fig 1B: courtesy of Emmanuel Baril (Ménagerie, le zoo du jardin de plantes, Paris).*

https://doi.org/10.1371/journal.pone.0254306.g001

beginning of the study. Echocardiographic variables (i.e., left atrial (LA) volumes, tricuspid annular plane systolic excursion (TAPSE)) were indexed based on the last recorded weight of the animals (one to four months before the study start).

The final TTE method was the following: trainers were always responsible for bringing BO to an appropriate place, the closest as possible to both the enclosure mesh and the observer. While they were distracting BO by gently and quietly talking to them and giving them some food, optimal acoustic windows were identified and obtained as promptly as possible by the observer, with the transducer placed through the enclosure mesh on BO thorax previously covered by coupling gel (**S1 Video**; **Fig 1**). Each examination was timed and systematically included four 2D views [8], i.e., the apical 4- and 5-chamber views, the parasternal short-axis view at the level of the aortic valve, and the apical long-axis view optimized for TAPSE measurement.

Apical 4-chamber-view (Figs 2 and 3). The apical 4-chamber was obtained as described in the GAHP report, with the probe placed on the left lateral portion of the chest at the apex of the heart [8].

M-mode echocardiograms showing at least five consecutive cardiac cycles were obtained for offline mitral annular motion measurement (**Fig 2A**) [9]. Pulsed-wave Doppler images were also obtained for offline assessment of peak velocity of early and late diastolic transmitral flows (E and A waves, respectively) and E wave deceleration time, with calculation of the E:A

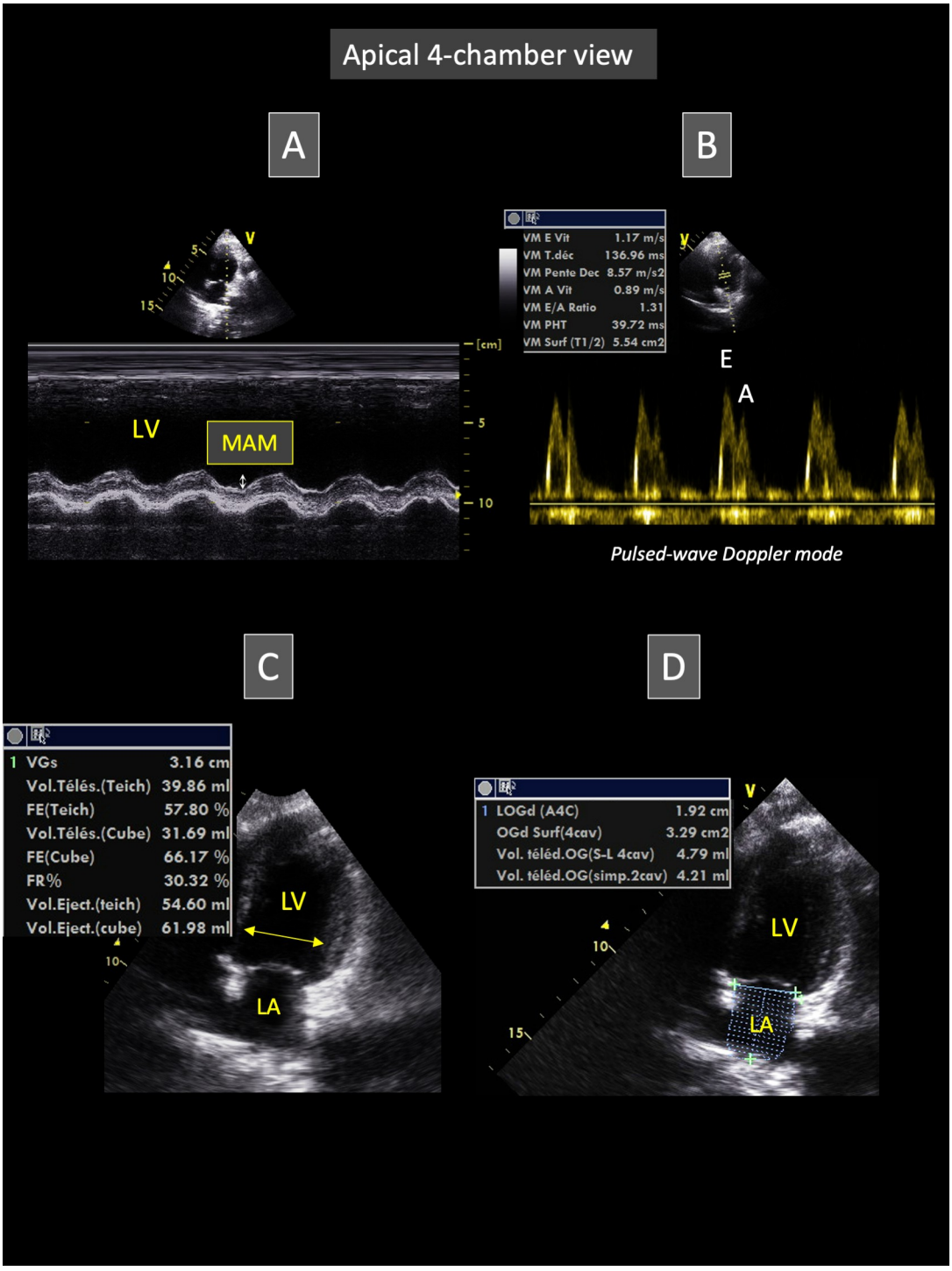

Fig 2. Representative apical 4-chamber view obtained from Borneo orangutans involved in the study. This view allows to place the M-mode cursor through the lateral mitral annulus for measurement of mitral annular motion (MAM, A) and to obtain transmitral flow recordings using pulsed-wave Doppler mode (B). Video loops of this view can also be used for left ventricular (C) and left atrial measurements (D). Fig 2C and 2D respectively show measurements of the end-systolic left ventricular diameter and end-diastolic left atrial volume (see text for explanation). *E and A*: *peak velocity of early and late diastolic transmitral flows*, *respectively; LA*: *left atrium; LV*: *left ventricle.*

https://doi.org/10.1371/journal.pone.0254306.g002

ratio (Fig 2B). As no arrhythmia was detected, heart rate was simply assessed by calculating the time interval between two consecutive peak velocities of early diastolic transmitral flow.

The apical 4-chamber view was also recorded as video loops including at least five consecutive cardiac cycles, that were digitally stored for offline analysis and assessment of left heart dimensions and function. The end-diastolic and end-systolic LV internal diameters were measured from inner edge to inner edge of the LV cavity (Fig 2C), perpendicular to myocardial walls, and just proximal to mitral leaflet tips at their maximal diastolic opening. End-diastole was defined as the frame showing the largest LV cavity after mitral valve closure, and end-systole as the last frame before mitral valve opening. The corresponding fractional shortening was then calculated. Additionally, the end-diastolic and end-systolic LV volumes were automatically assessed using the Simpson's method of discs by manually tracing the LV endocardial border at blood-tissue interface, from the septal mitral annulus, up to the apex, and then to the lateral mitral annulus, with exclusion of papillary muscles from the traced border [10]. Ventricular volumes were then used to calculate the LV ejection fraction as previously described [10]. From the same 2D loops of the apical 4-chamber view used to assess LV dimensions, the LA endocardial border was manually traced at end-systole and end-diastole, with exclusion of the left auricle and pulmonary veins from the traced border, to assess LA lengths and volumes using the Simpson's method of discs (Fig 2D) [11]. Left atrial volumes were then indexed to body weight.

Furthermore, maximal thickness of the anterior and posterior mitral valve leaflets was measured from the same 2D loops at their maximal diastolic opening.

Finally, the apical 4-chamber loops were also used to assess the STI longitudinal LV systolic strain (StS), as previously described (Fig 3) [12]. Briefly, the LV endocardial border was manually traced at end-diastole (corresponding to the largest LV cavity after mitral valve closure). A region of interest, in which the computer software (Echo Pac PC 6.3 software for Vivid 7, GE Healthcare) automatically performed speckle tracking, was drawn to include the entire myocardium, and the software algorithm then automatically segmented the LV myocardium into 6 segments (3 within the interventricular septum and 3 within the LV free wall). Six longitudinal StS profiles were thus obtained, and peak longitudinal StS values were automatically assessed for each of the 6 LV segments. The mean value of peak StS (corresponding to StS_{4chv}) was then calculated.

Apical 5-chamber-view (Figs 4 and 5). The apical 5-chamber view was obtained from the apical 4-chamber view as described in the GAHP report, by tilting and sliding the transducer beam cranially [8]. Continuous-wave and pulsed-wave Doppler images were obtained for offline calculation of aortic peak flow velocity and isovolumic relaxation time, respectively (Fig 4A). Additionally, the apical 5-chamber view was recorded as video loops including at least five consecutive cardiac cycles, that were digitally stored for offline analysis. Anatomic M-mode (AMM) images were generated from these digital 2D video loops. The electronic AMM cursor was carefully placed across the LA and the aortic root, perpendicular to the aortic and LA walls (Fig 4B). The LA end-systolic AMM diameter and the aortic end-diastolic AMM diameter were measured from inner edge to inner edge, and the corresponding LA:Aorta AMM ratio was then calculated.

The same video loops were used to assess the STI longitudinal LV StS (StS_{5chv}), as described above for StS_{4chv} (Fig 5). The global LV StS (StS_{global}) was assessed by calculating the mean of StS_{5chv} and StS_{4chv}.

Heart rate was assessed by calculating the time interval between two consecutive aortic peak flow velocities.

Parasternal short-axis view at the level of the aortic valve. The parasternal short-axis view at the level of the aortic valve was obtained as described in the GAHP report, with the

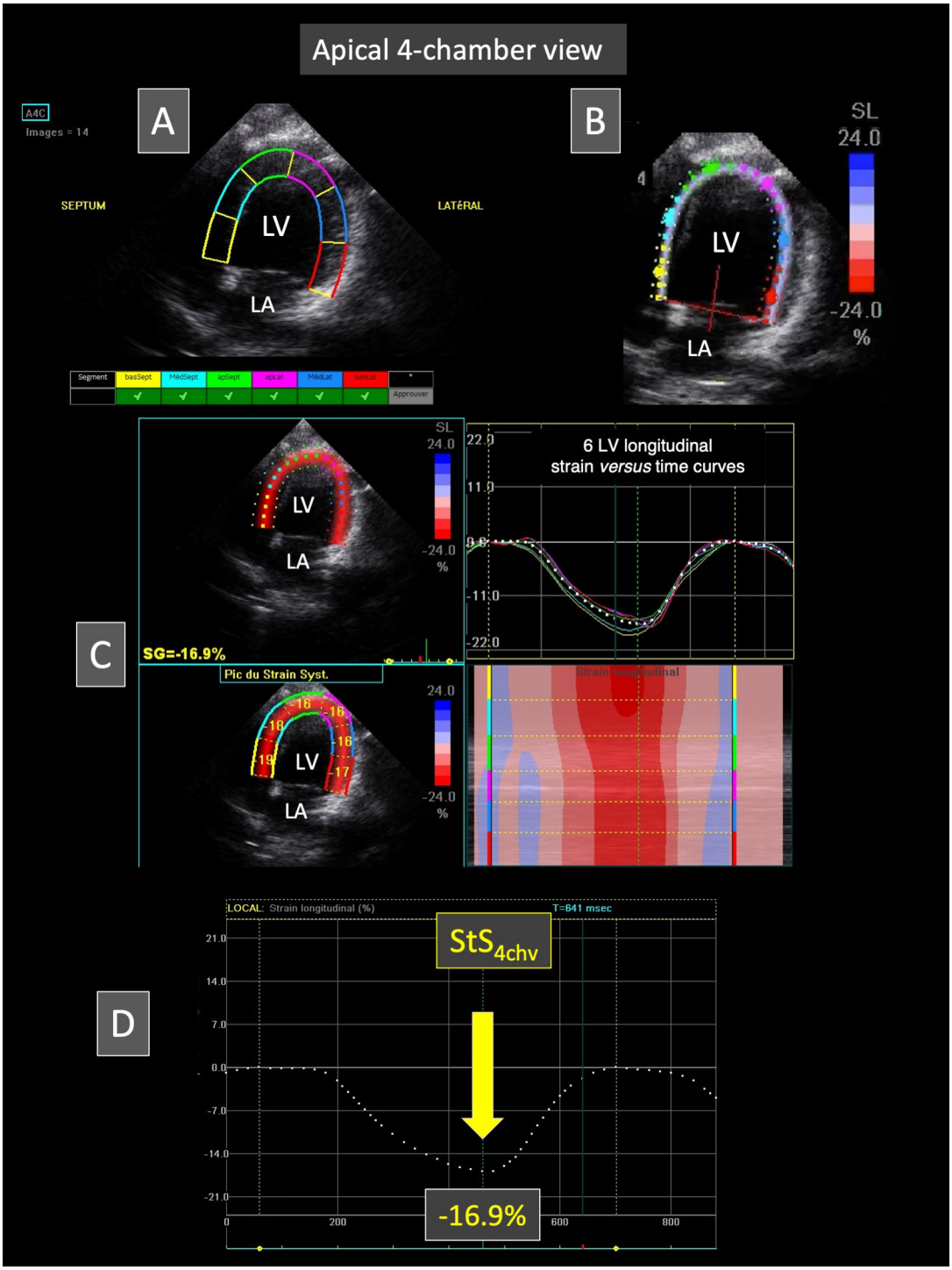

Fig 3. Representative speckle tracking imaging examination performed from the apical 4-chamber view in a Borneo orangutan. The left ventricular endocardial border is traced and a region of interest including left ventricular myocardial walls is automatically drawn (A). The software algorithm then automatically separates left ventricular myocardial walls into 6 equidistant segments (A and B). The tracking quality is displayed for each segment (A). Fig C shows on the right the 6 left ventricular longitudinal strain *versus* time curves (corresponding to the 6 myocardial segments) during a single cardiac cycle. This representative case demonstrates that all the 6 LV segments undergo a relatively homogenous systolic myocardial shortening during systole (negative strain). The corresponding color map below displays the change in strain over time in each segment during the same single cardiac cycle. The peak systolic strain is displayed in each of the six segments on the two-dimensional color-coded view (left). Fig D shows the mean left ventricular longitudinal strain *versus* time curve. In this case, the peak systolic strain value (StS_{4chv}) is—16.9%. *LA*: *left atrium; LV*: *left ventricle.*

https://doi.org/10.1371/journal.pone.0254306.g003

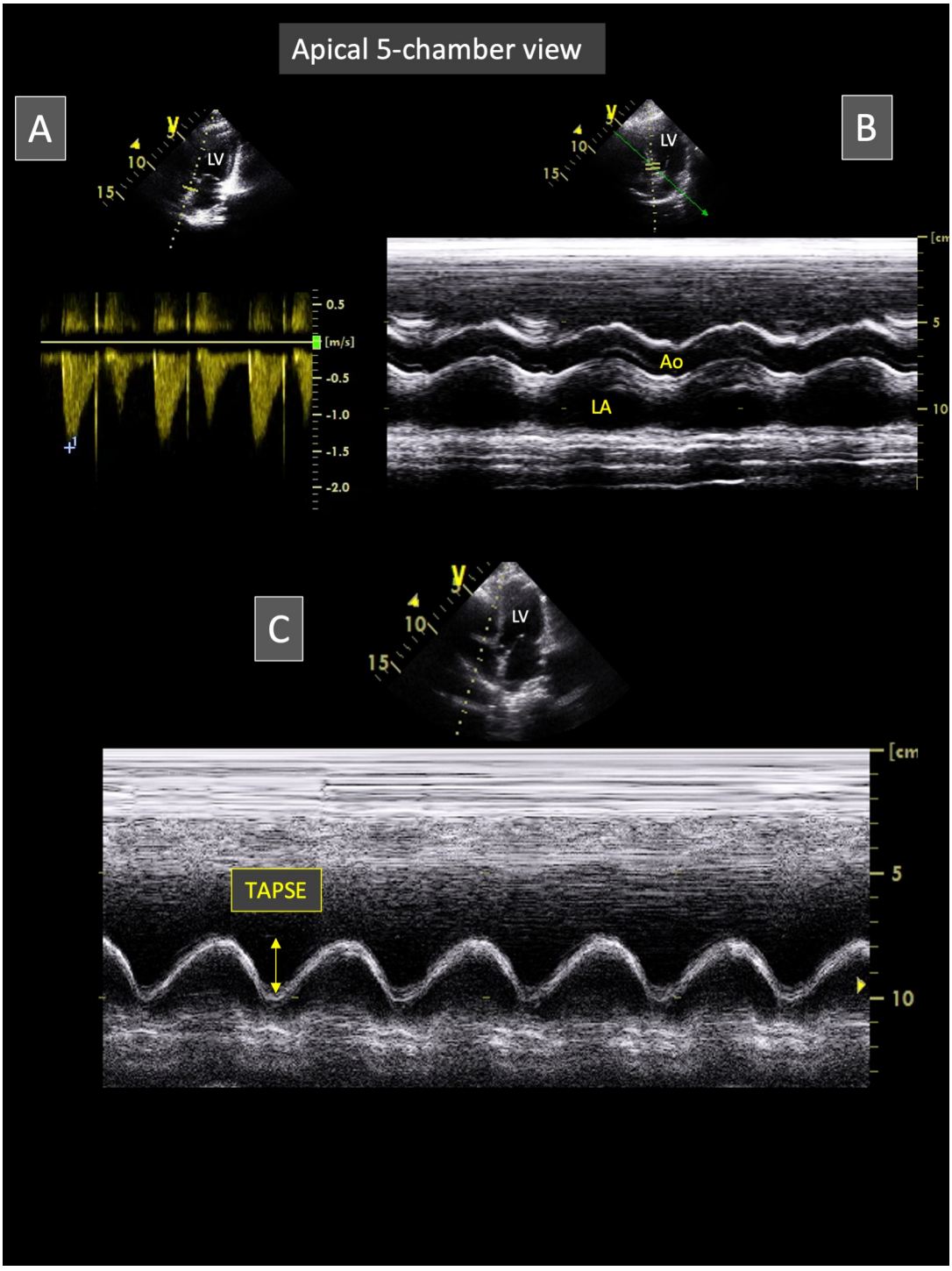

Fig 4. Representative apical 5-chamber view obtained from Borneo orangutans involved in the study. This view allows to obtain aortic flow recordings using continuous-wave Doppler mode (A). Video loops of this view can also be recorded for post-processing measurements of the left atrium and the aorta using the anatomic M-mode technique (B). For this purpose, the M-mode line is positioned perpendicular to left atrial and aortic walls (B). Lastly, by slightly tilting the probe from this position, the M-mode line can also be placed through the lateral segment of the tricuspid annulus for optimal measurement of the tricuspid annular plane systolic excursion (TAPSE; C). *Ao*: *aorta; LA*: *left atrium; LV*: *left ventricle*.

https://doi.org/10.1371/journal.pone.0254306.g004

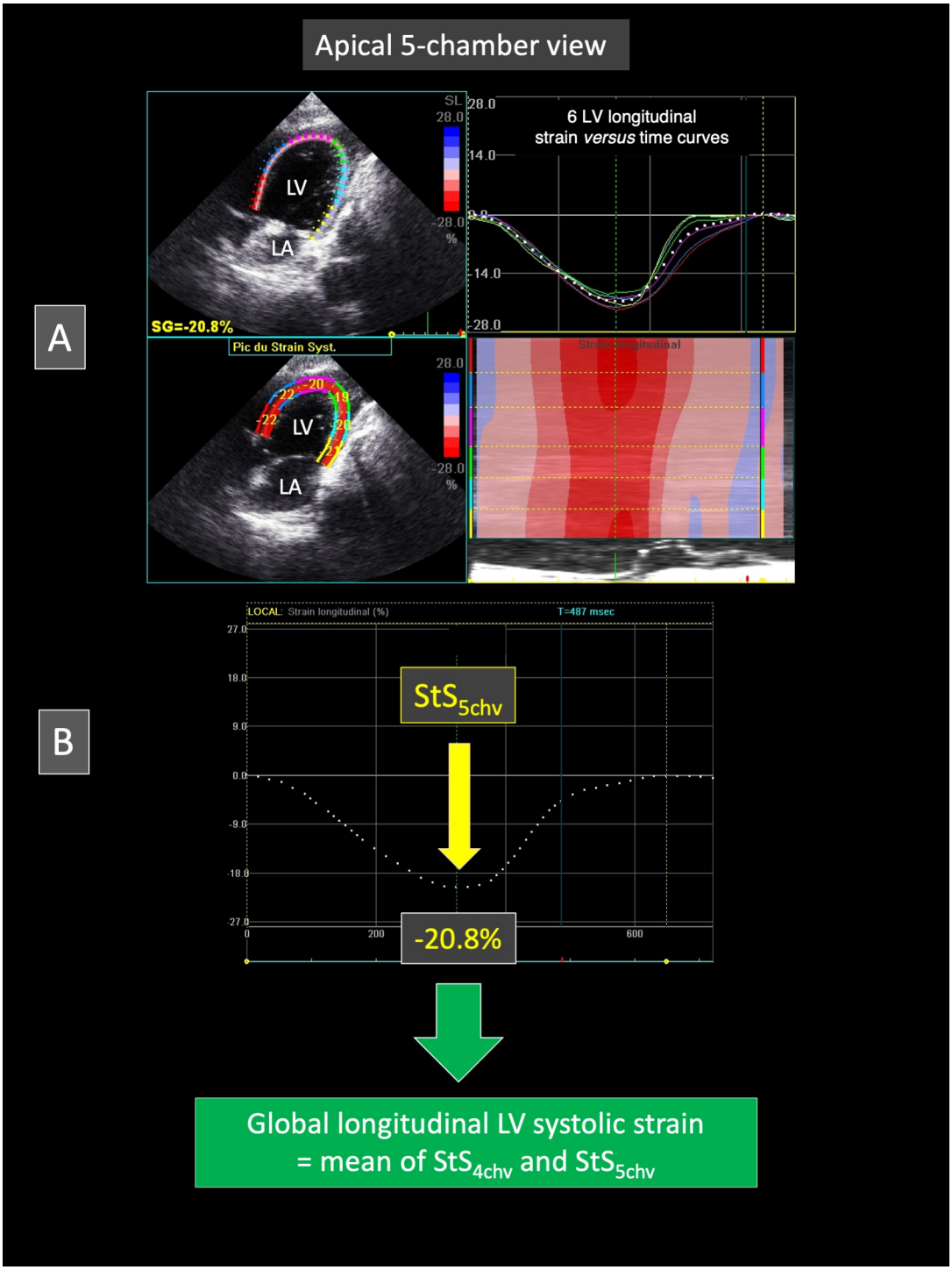

Fig 5. Representative speckle tracking imaging examination performed from the apical 5-chamber view in a Borneo orangutan. As described in Fig 3 for the apical 4-chamber view, the left ventricular endocardial border has been traced and a region of interest including left ventricular myocardial walls has been automatically drawn. Six equidistant myocardial segments have been defined. Fig A shows on the right the 6 left ventricular longitudinal strain *versus* time curves (corresponding to the 6 myocardial segments) during a single cardiac cycle. This representative case demonstrates that all the 6 LV segments undergo a relatively homogenous systolic myocardial shortening during systole (negative strain), with the corresponding color map below displaying the change in strain over time in each segment during the same single cardiac cycle, and with the peak systolic strain displayed in each segment on the two-dimensional color-coded view (left). Fig B shows the mean left ventricular longitudinal strain *versus* time curve. In this case, the peak systolic strain value (StS_{5chv}) is—20.8%. The global left ventricular systolic strain is

then assessed by averaging mean peak systolic strain values obtained from the apical 4- and 5-chamber view, i.e., StS_{4chv} and StS_{5chv}, respectively. *LA*: *left atrium; LV*: *left ventricle*.

https://doi.org/10.1371/journal.pone.0254306.g005

probe placed more cranially as compared to the two above-mentioned apical views, between the sternum and the left nipple [8]. Continuous-wave Doppler images were obtained for offline calculation of pulmonic peak flow velocity.

Apical long-axis view optimized for TAPSE measurement. M-mode echocardiograms showing at least five consecutive cardiac cycles were obtained using either apical 4- or 5-chamber view (**Fig 4C**), slightly modified for optimal visualization of the tricuspid annulus and offline TAPSE measurement. In addition, TAPSE values were indexed to body weight. Heart rate was assessed by calculating the time interval between two consecutive maximal tricuspid annular systolic excursions on M-mode echocardiograms.

Assessment of intra-observer within-day and between-day variability of TTE variables

A total of 96 echocardiographic examinations were performed on 4 different days over a 2.5-month period. Each BO was examined 6 times per day. As above-mentioned, each examination performed by the same trained observer included four two-dimensional (2D) views, with offline assessment of 28 variables. A general linear model was used to determine the within-day and between-day coefficients of variation (CV).

Statistical analysis

Data are expressed as mean ± standard deviation (SD). Statistical analyses were performed using a computer software (R Core Team (2018). R version 3.5.2: A language and environment for statistical computing. R Foundation for Statistical Computing, Vienna, Austria). Briefly, and as already described in our previous ultrasound imaging validation studies performed on wild or exotic animals [13, 14], the following linear model was used to analyze the within-day and between-day variability of the TTE variables:

$$Y_{ijk} = \mu + day_i + BO_j + (day \times BO)_{ij} + \varepsilon_{ijk}$$

where Y_{ijk} is the k^{th} value measured for BO j on day i, μ is the general mean, day_i is the differential effect of day i, BO_j is the differential effect of BO j, $(day \times BO)_{ij}$ is the interaction term between day and BO, and ε_{ijk} is the model error. The SD of repeatability was estimated as the residual SD of the model and the SD of reproducibility as the SD of the differential effect of day. The corresponding CV values were determined by dividing each SD by the mean. The level of significance was set at $P<0.05$.

Results

All 96 TTE examinations could be performed, with a mean image acquisition duration of 3.8 ± 1.6 minutes (1.3–6.3).

All of the 28 tested variables (i.e., 2D (n = 12), M-mode and anatomic M-mode (n = 6), Doppler (n = 7), and STI (n = 3)) could be assessed offline, representing a total of 2,688 measurements.

The mean heart rate ± SD during TTE examinations was 93 ± 9 beats per minute (76–118).

Tables 1 and **2** give the values for the 2,688 repeated TTE measurements, i.e., 2D, M-mode and AMM variables in **Table 1**, and Doppler and STI variables in **Table 2**. The corresponding within-day and between-day SD and CV values are shown in **Tables 3 and 4**, respectively.

Table 1. Mean ± standard deviation (SD), minimum (Min) and maximum (Max) values of repeated measurements of two-dimensional (n = 12), M-mode (n = 3) and anatomic M-mode (n = 3) echocardiographic variables (n = 18) obtained by a trained observer in 4 Borneo orangutans (*Pongo pygmaeus pygmaeus*) from 96 transthoracic examinations, BO1 to BO3 being the females and BO4 the male.

Echocardiographic parameters	Mean ± SD (Min—Max)	BO1	BO2	BO3	BO4
Apical 4-chamber view two-dimensional-parameters					
Left ventricular end-diastolic internal diameter (mm)	40.0 ± 4.3 (34.7–47.2)	37.0 ± 1.0 (35.5–39.0)	35.6 ± 0.6 (34.7–36.8)	41.4 ± 1.1 (40.0–43.4)	46.1 ± 0.7 (44.6–47.2)
Left ventricular end-systolic internal diameter (mm)	27.4 ± 3.0 (23.6–32.8)	25.3 ± 0.7 (24.5–27.4)	24.3 ± 0.5 (23.6–25.3)	28.3 ± 0.9 (26.8–30.0)	31.6 ± 0.7 (30.2–32.8)
Left ventricular radial fractional shortening (%)	31.5 ± 1.9 (20.8–34.6)	31.7 ± 1.0 (30.1–33.7)	31.8 ± 1.2 (30.0–33.8)	31.1 ± 2.5 (20.8–34.2)	31.4 ± 1.1 (30.1–34.6)
Left ventricular ejection fraction (%)	52.6 ± 8.4 (40.0–69.0)	45.0 ± 2.9 (40.0–49.0)	64.3 ± 2.7 (59.0–69.0)	54.6 ± 3.0 (47.0–60.0)	46.3 ± 2.0 (43.0–52.0)
Left atrial end-diastolic length (cm)	2.09 ± 0.27 (1.50–2.80)	2.11 ± 0.16 (1.80–2.40)	1.93 ± 0.16 (1.60–2.20)	2.37 ± 0.23 (1.90–2.80)	1.94 ± 0.17 (1.50–2.20)
Left atrial end-systolic length (cm)	3.07 ± 0.36 (2.40–3.90)	3.34 ± 0.15 (3.00–3.60)	2.95 ± 0.18 (2.60–3.20)	3.35 ± 0.25 (2.80–3.90)	2.65 ± 0.15 (2.40–2.90)
Left atrial end-diastolic volume (mL)	5.8 ± 1.7 (3.1–8.9)	5.2 ± 0.3 (4.7–5.8)	3.5 ± 0.3 (3.1–4.0)	7.9 ± 0.5 (7.0–8.9)	6.4 ± 0.3 (6.0–6.9)
Left atrial end-diastolic volume indexed to body weight (mL/kg)	0.09 ± 0.02 (0.06–0.13)	0.07 ± 0.00 (0.06–0.08)	0.08 ± 0.01 (0.07–0.08)	0.12 ± 0.01 (0.10–0.13)	0.12 ± 0.01 (0.11–0.13)
Left atrial end-systolic volume (mL)	17.5 ± 3.6 (13.0–23.6)	20.2 ± 0.8 (19.1–21.5)	13.8 ± 0.6 (13.0–14.9)	21.7 ± 1.2 (19.6–23.6)	14.4 ± 0.5 (13.6–15.2)
Left atrial end-systolic volume indexed to body weight (mL/kg)	0.29 ± 0.02 (0.25–0.34)	0.27 ± 0.01 (0.26–0.29)	0.29 ± 0.01 (0.28–0.32)	0.32 ± 0.02 (0.29–0.34)	0.26 ± 0.01 (0.25–0.28)
Maximal thickness of the anterior mitral valve leaflet (mm)	3.2 ± 0.6 (2.3–4.3)	2.7 ± 0.2 (2.3–2.9)	2.7 ± 0.2 (2.3–2.9)	3.5 ± 0.2 (3.1–3.8)	4.1 ± 0.1 (3.9–4.3)
Maximal thickness of the posterior mitral valve leaflet (mm)	3.2 ± 0.7 (2.1–4.4)	2.7 ± 0.2 (2.4–3.1)	2.6 ± 0.2 (2.1–2.9)	3.4 ± 0.2 (3.1–3.9)	4.2 ± 0.1 (4.0–4.4)
Apical 4-chamber view M-mode parameter					
Mitral annular motion (cm)	1.45 ± 0.10 (1.28–1.60)	1.53 ± 0.04 (1.50–1.60)	1.42 ± 0.06 (1.30–1.60)	1.34 ± 0.05 (1.28–1.50)	1.52 ± 0.06 (1.40–1.60)
Apical 5-chamber view M-mode and anatomic M-mode parameters					
Left atrial end-systolic diameter (cm)	2.83 ± 0.38 (2.33–3.51)	2.97 ± 0.11 (2.81–3.30)	2.55 ± 0.05 (2.41–2.65)	3.35 ± 0.13 (3.04–3.51)	2.43 ± 0.05 (2.33–2.54)
Aortic end-diastolic diameter (cm)	2.28 ± 0.25 (1.08–2.54)	2.43 ± 0.03 (2.36–2.49)	1.97 ± 0.19 (1.08–2.07)	2.44 ± 0.05 (2.34–2.54)	2.30 ± 0.03 (2.24–2.35)
Left atrium/aorta ratio	1.24 ± 0.20 (1.02–2.38)	1.22 ± 0.05 (1.15–1.38)	1.32 ± 0.23 (1.21–2.38)	1.37 ± 0.06 (1.23–1.45)	1.06 ± 0.02 (1.02–1.09)
Tricuspid annular plane systolic excursion (cm)	2.55 ± 0.38 (1.90–3.20)	2.92 ± 0.10 (2.80–3.10)	2.04 ± 0.10 (1.90–2.20)	2.84 ± 0.15 (2.70–3.20)	2.42 ± 0.06 (2.30–2.50)
Tricuspid annular plane systolic excursion indexed to body weight (mm/kg)	0.42 ± 0.02 (0.38–0.47)	0.39 ± 0.01 (0.38–0.42)	0.43 ± 0.02 (0.40–0.47)	0.41 ± 0.02 (0.39–0.47)	0.44 ± 0.01 (0.42–0.46)

https://doi.org/10.1371/journal.pone.0254306.t001

Nearly all within-day and between-day CV values (55/56, 98%) were <15%, except for the between-day CV value of the end-diastolic left atrial length (16.8%).

Most within-day and between-day CV values (51/56, 91%) were <10%, including those of STI StS variables (2.7% to 5.4%), the lowest being observed for the end-diastolic LV internal diameter (2.2% and 2.9% for within- and between-day CV values, respectively).

A significant BO effect was observed for all TTE variables ($P<0.05$), except for the LV fractional shortening ($P = 0.33$). No significant day effect was observed for all of the 28 tested variables, except for the less reproductible one, i.e., the end-diastolic left atrial length ($P = 0.04$), and for the peak aortic flow velocity ($P = 0.03$).

Table 2. Mean ± standard deviation (SD), minimum and maximum values of repeated measurements of Doppler (n = 7) and STE (n = 3) variables (n = 10) obtained by a trained observer in 4 Borneo orangutans (*Pongo pygmaeus pygmaeus*) from 96 transthoracic examinations.

Echocardiographic parameters	Mean ± SD	Minimum—Maximum
Doppler parameters		
Peak velocity of early diastolic transmitral flow (E wave) (m/s)	1.19 ± 0.10	1.04–1.42
Peak velocity of late diastolic transmitral flow (A wave) (m/s)	0.61 ± 0.20	0.30–0.94
E:A ratio	2.21 ± 0.79	1.20–3.70
E wave deceleration time (ms)	125.7 ± 13.8	101.0–166.0
Aortic peak flow velocity (m/s)	1.52 ± 0.12	1.30–1.77
Isovolumic relaxation time (ms)	76.3 ± 17.2	50.0–104.0
Pulmonic peak flow velocity (m/s)	1.25 ± 0.10	1.07–1.45
Speckle tracking imaging parameters		
Longitudinal left ventricular systolic strain (4-chamber view) x -1 (%)	16.3 ± 0.7	14.7–17.8
Longitudinal left ventricular systolic strain (5-chamber view) x -1 (%)	18.1 ± 1.3	15.9–20.8
Global left ventricular systolic strain x -1 (%)	17.2 ± 0.6	16.1–18.4

https://doi.org/10.1371/journal.pone.0254306.t002

Discussion

Knowledge of cardiology in BO is scarce. To the best of the authors' knowledge, no study has yet provided quantitative data on heart morphology and function in awake BO, and LV

Table 3. Within-day and between-day variability, expressed as standard deviations (SD) and coefficients of variation (CV), of two-dimensional (n = 12), M-mode (n = 3) and anatomic M-mode (n = 3) echocardiographic variables (n = 18) obtained by a trained observer in 4 Borneo orangutans (*Pongo pygmaeus pygmaeus*) from 96 transthoracic examinations.

Echocardiographic parameters	Within-day		Between-day	
	SD	CV (%)	SD	CV (%)
Apical 4-chamber view two-dimensional-parameters				
Left ventricular end-diastolic internal diameter (mm)	0.88	2.20	1.17	2.94
Left ventricular end-systolic internal diameter (mm)	0.70	2.57	1.18	4.30
Left ventricular radial fractional shortening (%)	1.57	4.99	1.88	5.98
Left ventricular ejection fraction (%)	2.68	5.10	3.81	7.26
Left atrial end-diastolic length (cm)	0.18	8.43	0.35	16.78
Left atrial end-systolic length (cm)	0.19	6.10	0.28	9.07
Left atrial end-diastolic volume (mL)	0.36	6.27	0.39	6.79
Left atrial end-diastolic volume indexed to body weight (mL/kg)	0.01	6.23	0.01	7.10
Left atrial end-systolic volume (mL)	0.78	4.48	1.27	7.25
Left atrial end-systolic volume indexed to body weight (mL/kg)	0.01	4.33	0.02	7.01
Maximal thickness of the anterior mitral valve leaflet (mm)	0.16	4.81	0.24	7.34
Maximal thickness of the posterior mitral valve leaflet (mm)	0.19	5.96	0.32	10.08
Apical 4-chamber view M-mode parameter				
Mitral annular motion (cm)	0.05	3.66	0.08	5.75
Apical 5-chamber view anatomic M-mode parameters				
Left atrial end-systolic diameter (cm)	0.09	3.13	0.13	4.68
Aortic end-diastolic diameter (cm)	0.10	4.45	0.16	7.04
Left atrium/aorta ratio	0.12	9.73	0.18	14.82
Apical long-axis view optimized for M-mode tricuspid annular plane systolic excursion measurement				
Tricuspid annular plane systolic excursion (cm)	0.11	4.10	0.18	7.15
Tricuspid annular plane systolic excursion indexed to body weight (mm/kg)	0.02	4.11	0.03	6.44

https://doi.org/10.1371/journal.pone.0254306.t003

Table 4. Within-day and between-day variability, expressed as standard deviations (SD) and coefficients of variation (CV), of Doppler (n = 7) and STE (n = 3) variables (n = 10) obtained by a trained observer in 4 Borneo orangutans (*Pongo pygmaeus pygmaeus*) from 96 transthoracic examinations.

Echocardiographic parameters	Within-day		Between-day	
	SD	CV (%)	SD	CV (%)
Doppler parameters				
Peak velocity of early diastolic transmitral flow (E wave) (m/s)	0.03	2.46	0.04	3.29
Peak velocity of late diastolic transmitral flow (A wave) (m/s)	0.04	6.40	0.07	12.05
E:A ratio	0.17	7.54	0.30	13.43
E wave deceleration time (ms)	5.80	4.62	10.17	8.09
Aortic peak flow velocity (m/s)	0.04	2.33	0.07	4.79
Isovolumic relaxation time (ms)	2.76	3.62	3.68	4.83
Pulmonic peak flow velocity (m/s)	0.04	3.29	0.06	4.79
Speckle tracking imaging parameters				
Longitudinal left ventricular systolic strain (4-chamber view) x -1 (%)	0.66	4.04	0.89	5.44
Longitudinal left ventricular systolic strain (5-chamber view) x -1 (%)	0.67	3.70	0.87	4.82
Global longitudinal left ventricular systolic strain (%)	0.46	2.68	0.73	4.26

https://doi.org/10.1371/journal.pone.0254306.t004

myocardial function has never been quantitatively evaluated using STI in great apes. As optimal diagnostic techniques require precision (e.g., repeatability and reproducibility), accuracy, specificity, and sensitivity, the present study has investigated the feasibility and variability of TTE including STI in awake BO. This non-invasive and non-stressful imaging approach represents an essential initial step in the development of valuable diagnostic tools for the non-invasive *antemortem* diagnosis and longitudinal follow-up of BO heart diseases.

Borneo orangutans are classified as critically endangered according to the International Union for the Conservation of Nature [15]. Main causes of BO population decline include habitat destruction (deforestation, bushfire), illegal hunting, climate change, and lack of awareness of local populations [15]. As a result, captive BO are of major importance to increase public awareness and raise funds for their conservation, and also to act as a potential source of repopulation [4]. Captive BO population management is hence essential to maintain healthy individuals under managed care, and in this context any disease can be considered as a threat [4]. Cardiovascular diseases are a major cause of morbidity and mortality in all great ape taxa, accounting for up to 20%, 38%, 41%, and 45% of deaths in captive orangutans (*Pongo spp*.), chimpanzees (*Pan troglotydes*), gorillas (*Gorilla spp*.), and bonobos (*Pan paniscus*), respectively [1]. Transthoracic echocardiography could therefore represent a useful non-invasive tool for early diagnosis and routine follow-ups of great ape heart diseases. Additionally, TTE could allow a better understanding of these pathological conditions, including their etiology and pathogenesis, which would be key to the conservation of these species.

Due to the various disadvantages of general anesthesia which limit the use of TTE as a routine diagnostic tool (e.g., alterations of cardiac function, risk of complications) [8], the present report was specifically dedicated to developing a method for TTE in awake BO. Developing such approach is of particular interest, as health issues, namely respiratory infectious diseases, appear to be of specific concern in BO [16], which may increase anesthetic risks.

The innovative veterinary program called the GAHP has provided guidelines for TTE in great apes, with suggestions for standardization of nomenclature, cardiac imaging views, and measurements [8]. Several views have thus been identified and described, i.e., three parasternal long axis views, three parasternal short-axis views, three apical views (apical 5-, 4- and 2-chamber views), and also one suprasternal and one subcostal view. The objective of the present study was to develop a TTE method in awake BO, that should ideally be non-stressful for the

animals and as safe as possible for involved observers, trainers, and equipment. Therefore, time for image acquisition had to be as short as possible. For this purpose, the present protocol focused on a minimal number of views (i.e., four echocardiographic views only), chosen to provide a wide range of quantitative variables for the assessment of heart dimensions and function using 2D and M-mode echocardiography, spectral Doppler, and STI, with all measurements performed after TTE sessions. Using the proposed method, a total of 28 variables of interest could be assessed offline, requiring a limited image acquisition duration, i.e., mean and maximal duration of respectively 3.8 and 6.3 minutes, only. The apical 4- and 5-chamber views provided the largest number of quantitative variables. Interestingly, one single video loop of the apical 4-chamber view allowed the post-processing assessment of 12 2D variables (LA and LV diameters and volumes, LV systolic indices, mitral valve leaflets thicknesses) as well as one STI longitudinal LV StS variable (StS_{4chv}). Similarly, one single video loop of the apical 5-chamber view allowed the post-processing assessment of three anatomic M-mode variables (LA and aortic diameters, LA:aorta ratio) as well as one STI longitudinal LV StS variable (StS_{5chv}), with then calculation of the global LV StS (as the mean of StS_{5chv} and StS_{4chv}). To summarize, a total of 18 variables could be assessed using only two video loops of apical views. The other 10 of the 28 tested imaging variables were technically more challenging because they needed the pre-processing placement of either the M-mode cursor (for mitral annular motion, TAPSE, and indexed TAPSE measurements) or the sample volume and Doppler cursor for spectral Doppler variables (regarding diastolic transmitral flow and systolic arterial flows). Unlike for systolic arterial flows, pulsed-wave Doppler mode was used for transmitral flow assessment, as this is the spectral Doppler mode recommended to evaluate LV diastolic function, which may be altered in the case of myocardial fibrosis [17] (and fibrosing cardiomyopathy represents the most common heart disease in BO [1]). All within-day and between-day CV values of M-mode variables were $<10\%$, and all those of spectral Doppler variables were $<15\%$, with only two between-day CV values between 10 and 15% (12.1% and 13.4% for mitral A wave and mitral E:A ratio, respectively), which corresponds to good to excellent repeatability and reproducibility.

The present study also shows that all within-day and between-day CV values of STI variables were $<10\%$. This is of particular interest as myocardial diseases, mainly including fibrosing cardiomyopathy and myocarditis, represent the most common orangutan heart diseases [1, 4–6]. The ability of STI to early detect systolic myocardial dysfunction has been demonstrated in human patients with various subclinical myocardial diseases characterized by normal conventional echocardiographic parameters (including LV diameters, fractional shortening, and ejection fraction) [18, 19]. We can therefore hypothesize that STI combined with spectral Doppler parameters of diastolic function could be useful for the early detection of myocardial diseases in captive BO.

In the present report, a significant BO effect was observed for all TTE variables, except for the LV fractional shortening. This result may be explained by the wide range of age (12 to 51 years old) and body weight (47 to 74 kg) of the four involved BO. As already described in the GAPH report [8], because orangutans vary in body shape and size, the optimal acoustic windows are slightly different from one animal to another. Additionally, among the four BO involved in the present study, the oldest female had the most prominent breast, making the transducer placement and images acquisition less easy. Finally, the four BO had variably developed laryngeal air sacs. These anatomical structures, typically extending along the ventral neck, beneath the clavicles and into the axilla, are involved in BO vocalization and communication [1]. Depending on their size, they may interfere with the ultrasound beam and variably alter the TTE image quality [8].

This preliminary work on TTE in BO presents several limitations. Neither cardiac auscultation nor diagnostic tests were performed on BO at inclusion in the study to confirm healthy condition of the animals (thus considered as "apparently healthy"). Color-flow Doppler mode was not used to rule out the presence of valve regurgitation or other potential abnormal flows (as this was not on the scope of the present study whose aim was to develop and assess the feasibility and variability of a non-stressful TTE method using quantitative variables). Quantitative measurements were limited to the left heart and aorta, as these were the easiest to detect and analyze. The right heart size was not evaluated, and TAPSE (indexed or not to body weight) was the only right ventricular function tested parameter. Additionally our previous studies in dogs and cats showed that TTE is a highly observer-dependent examination [20, 21]. The results presented here are thus only valid for the observer involved, and the authors encourage veterinarians to determine their own TTE variability, before undertaking further echocardiographic studies in BO or other great apes.

Conclusions

In conclusion, our results demonstrate that TTE can be performed in awake BO after three months of animal training, providing the assessment of more than 20 2D, M-mode, spectral Doppler, and STI variables with good to excellent repeatability and reproducibility as well as minimal animal restraint. The non-stressful nature of the present method relies on several factors including the use of positive reinforcement for BO training to the technique, and rapidity of image acquisition (mean duration of 4 minutes), as only four 2D views are required, with subsequent offline post-processing analysis. This TTE method may be useful for longitudinal follow-up of heart morphology and function in awake BO, which is of particular interest as cardiovascular diseases (e.g., congenital cardiac defects, myocarditis, and cardiomyopathies including fibrosing cardiomyopathy) have been identified as a major cause of mortality and morbidity in this endangered species. One can also speculate that this TTE method could be tested and applied to other great apes, which could be of practical interest as all taxa are known to be highly predisposed to heart diseases [8].

Supporting information

S1 Video. Video showing one of the Borneo orangutans (Pongo pygmaeus pygmaeus) involved in the study. The animal is sitting and presenting its chest to the trainer against the enclosure mesh with its arms raised, for recording transthoracic echocardiographic images and video loops. The transducer is placed by the observer through the enclosure mesh, after generously applying coupling gel to the acoustic window, while the trainer is talking and feeding the orangutan.
(MP4)

Acknowledgments

The authors would like to thank the Ménagerie, le Zoo du Jardin des Plantes staff for their collaboration in this study.

Author Contributions

Conceptualization: Valérie Chetboul, Didier Concordet, Norin Chai.

Data curation: Valérie Chetboul, Irène Vonfeld, Camille Poissonnier, Maria Paz Alvarado, Peggy Passavin, Mathilde Gluntz, Solène Lefort, Aude Bourgeois, Dylan Duby, Christelle Hano, Norin Chai.

Formal analysis: Didier Concordet, Renaud Tissier.

Investigation: Valérie Chetboul.

Methodology: Valérie Chetboul.

Project administration: Valérie Chetboul.

Supervision: Valérie Chetboul.

Validation: Valérie Chetboul.

Writing – original draft: Valérie Chetboul, Irène Vonfeld.

Writing – review & editing: Valérie Chetboul, Didier Concordet, Renaud Tissier, Irène Vonfeld, Camille Poissonnier, Maria Paz Alvarado, Peggy Passavin, Mathilde Gluntz, Solène Lefort, Aude Bourgeois, Dylan Duby, Christelle Hano, Norin Chai.

References

1. Lowenstine L. Cardiovascular disease in great apes. In: Fowler M, Miller R, editors. Fowler's Zoo and Wild Animal Medicine: Current Therapy. Saint Louis: Elsevier Inc; 2011. pp. 408–415.
2. Greenberg MJ, Janssen DL, Jamieson SW, Rothman A, Frankville DD, Cooper SD, et al. Surgical repair of an atrial septal defect in a juvenile Sumatran orangutan (*Pongo pygmaeus sumatraensis*). J Zoo Wildl Med. 1999; 30(2):256–261. PMID: 10484142
3. Cook RA, Sheppardson P, McGinn M, Roskop ML, Wong BY. Evaluation of a ventricular septal defect in an orangutan: a case report. J Med Primatol. 1986; 15(4):303–308. PMID: 3746889
4. Strong V, Martin M, Redrobe S, White K, Baiker K. A retrospective review of great ape cardiovascular disease epidemiology and pathology. Int Zoo Yearb. 2018; 52(1):113–125.
5. Miyagi J, Tsuhako K, Kinjo T, Iwamasa T, Kamada Y, Kinju T, et al. Coxsackievirus B myocarditis in an orangutan. Vet Pathol. 1999; 36(5):452–456. https://doi.org/10.1354/vp.36-5-452 PMID: 10490214
6. Yeo DSY, Lian JE, Fernandez CJ, Lin YN, Liaw JCW, Soh ML, et al. A highly divergent Encephalomyocarditis virus isolated from nonhuman primates in Singapore. Virol J. 2013; 10:248. https://doi.org/10.1186/1743-422X-10-248 PMID: 23914943
7. Chetboul V. Advanced techniques in echocardiography in small animals. Vet Clin North Am Small Anim Pract. 2010; 40(4):529–543. https://doi.org/10.1016/j.cvsm.2010.03.007 PMID: 20610009
8. Boyd R, Danforth M, Rapoport G, Sleeper M, Devlin W, Kutinsky I, et al. Great ape heart project guidelines for the echocardiographic assessment of great apes. J Zoo Wildl Med. 2020; 50(4):822–836. https://doi.org/10.1638/2018-0164 PMID: 31926512
9. Schober KE, Luis Fuentes V. Mitral annulus motion as determined by M-mode echocardiography in normal dogs and dogs with cardiac disease. Radiol Ultrasound. 2001; 42(1):52–61. https://doi.org/10.1111/j.1740-8261.2001.tb00904.x PMID: 11245239
10. Serres F, Chetboul V, Tissier R, Poujol L, Gouni V, Carlos Sampedrano C, et al. Comparison of 3 ultrasound methods for quantifying left ventricular systolic function: correlation with disease severity and prognostic value in dogs with mitral valve disease. J Vet Intern Med. 2008; 22(3):566–577. https://doi.org/10.1111/j.1939-1676.2008.0097.x PMID: 18466240
11. Tidholm A, Bodegård-Westling A, Höglund K, Häggström J, Ljungvall I. Comparison between real-time 3-dimensional and 2-dimensional biplane echocardiographic assessment of left atrial volumes in dogs with myxomatous mitral valve disease. J Vet Intern Med. 2019; 33(2):455–461. https://doi.org/10.1111/jvim.15408 PMID: 30628129
12. Chetboul V, Damoiseaux C, Lefebvre HP, Concordet D, Desquilbet L, Gouni V, et al. Quantitative assessment of systolic and diastolic right ventricular function by echocardiography and speckle-tracking imaging: a prospective study in 104 dogs. J Vet Sci. 2018; 19(5):683–692. https://doi.org/10.4142/jvs.2018.19.5.683 PMID: 30041288
13. Chetboul V, Lichtenberger J, Mellin M, Mercera B, Hoffmann AC, Chaix G, et al. Within-day and between-day variability of transthoracic anatomic M-mode echocardiography in the awake bottlenose

dolphin (*Tursiops truncatus*). J Vet Cardiol. 2012; 14(4):511–518. https://doi.org/10.1016/j.jvc.2012.07.002 PMID: 23102806

14. Chetboul V, Gouni V, Tissier R, Jiménez Soto M, Huynh M, Pouchelon J-L, et al. Feasibility, within-day and between-day variability of transthoracic echocardiography in sloths (*Bradypus variegatus* and *Choloepus hoffmanni*): A Pilot Study. J Vet Sci Med Diagn. 2017; 6:1–6.
15. Ancrenaz M, Gumal M, Marshall AJ, Meijaard E, Wich SA, Husson S. Pongo pygmaeus (errata version published in 2018). In: The IUCN Red List of Threatened Species 2016: e.T17975A123809220 2016; downloaded on 10 May 2021. https://doi.org/10.2305/IUCN.UK.2016-1.RLTS.T17975A17966347.en
16. Zimmermann N, Pirovino M, Zingg R, Clauss M, Kaup FJ, Heistermann M, et al. Upper respiratory tract disease in captive orangutans (Pongo sp.): prevalence in 20 European zoos and predisposing factors. J Med Primatol. 2011; 40(6):365–375. https://doi.org/10.1111/j.1600-0684.2011.00490.x PMID: 21770970
17. Nagueh SF, Smiseth OA, Appleton CP, Byrd BF 3rd, Dokainish H, Edvardsen T, et al. Recommendations for the evaluation of left ventricular diastolic function by echocardiography: an update from the American Society of Echocardiography and the European Association of Cardiovascular Imaging. J Am Soc Echocardiogr. 2016; 29(4):277–314. https://doi.org/10.1016/j.echo.2016.01.011 PMID: 27037982
18. Song G, Zhang J, Wang X, Zhang X, Sun F, Yu X. Usefulness of speckle-tracking echocardiography for early detection in children with Duchenne muscular dystrophy: a meta-analysis and trial sequential analysis. Cardiovasc Ultrasound. 2020; 18(1):26. https://doi.org/10.1186/s12947-020-00209-y PMID: 32650783
19. Van der Bijl P, Bootsma M, Hiemstra YL, Ajmone Marsan N, Bax JJ, Delgado V. Left ventricular 2D speckle tracking echocardiography for detection of systolic dysfunction in genetic, dilated cardiomyopathies. Eur Heart J Cardiovasc Imaging. 2019; 20(6):694–699. https://doi.org/10.1093/ehjci/jey169 PMID: 30445576
20. Chetboul V, Concordet D, Pouchelon JL, Athanassiadis N, Muller C, Benigni L, et al. Effects of inter- and intra-observer variability on echocardiographic measurements in awake cats. J Vet Med A Physiol Pathol Clin Med. 2003; 50(6):326–331. https://doi.org/10.1046/j.1439-0442.2003.00546.x PMID: 12887627
21. Chetboul V, Athanassiadis N, Concordet D, Nicolle A, Tessier D, Castagnet M, et al. Observer-dependent variability of quantitative clinical endpoints: the example of canine echocardiography. J Vet Pharmacol Ther. 2004; 27(1):49–56. https://doi.org/10.1046/j.0140-7783.2003.00543.x PMID: 14995967